IJPSR (2026), Volume 17, Issue 1 (Research Article)

INTERNATIONAL JOURNAL OF PHARMACEUTICAL SCIENCES AND RESEARCH

Received on 04 July 2025; received in revised form, 01 August 2025; accepted, 05 August 2025; published 01 January 2026

TARGETING DIHYDROFOLATE REDUCTASE (DHFR) ENZYME: SYNTHESIS, *IN-VITRO* BIOLOGICAL EVALUATION, AND MOLECULAR MODELLING OF NOVEL TETRAHYDROPYRIMIDINE AND DIHYDROPYRIDINE DERIVATIVES

Menna M. Sherif [*1], Basem Mansour [1, 2], May A. El-Antrawy [3], Sahar M. I. Badr [4] and Magda. N. A. Nasr [4, 5]

Department of Pharmaceutical Chemistry [1], Faculty of Pharmacy, Delta University for Science and Technology, Gamasa 35712, Dakahlia, Egypt.
Department of Pharmaceutical Chemistry [2], University of Kut, Kut, Wasit, 52001 Iraq.
Department of Microbiology and Biotechnology [3], Faculty of Pharmacy, Delta University for Science and Technology, Gamasa 35712, Dakahlia, Egypt.
Department of Pharmaceutical Organic Chemistry [4], Faculty of Pharmacy, Mansoura University, Mansoura, 35516, Egypt.
Department of Pharmaceutical Organic Chemistry [5], Faculty of Pharmacy, Horus University-Egypt, New Damietta, 34518, Egypt.

Keywords:

DHFR, Tetrahydropyrimidine, Pyridine, Levofloxacin, Molecular Modelling

Correspondence to Author:
Menna M. Sherif

Department of Pharmaceutical Chemistry, Faculty of Pharmacy, Delta University for Science and Technology, Gamasa 35712, Dakahlia, Egypt.

E-mail: mennatallahsherif0@gmail.com

ABSTRACT: The increasing prevalence of multidrug-resistant (MDR) pathogens has severely undermined the efficacy of conventional antibiotics, necessitating the development of novel antimicrobial agents. Dihydrofolate reductase (DHFR), a crucial enzyme in bacterial DNA synthesis, presents a validated target for the design of new antimicrobial therapies. In this study, a new series of pyrazolyl-pyrimidine and pyridine-based derivatives was synthesized and systematically evaluated for DHFR inhibition and antimicrobial activity. The compounds were screened against a panel of pathogenic microorganisms, including *Escherichia coli*, *Klebsiella pneumoniae*, *Staphylococcus aureus*, and *Candida albicans*. Notably, compound 4c emerged as a lead molecule, displaying excellent antimicrobial potency with MIC values of 16 µg/mL against *S. aureus* and *C. albicans*. Additionally, it demonstrated a potent inhibitory effect on DHFR (IC50 = 5.53 ± 0.26 µM) and achieved a docking score of –12.114 kcal/mol, indicating strong binding affinity. Structure-activity relationship (SAR) analysis revealed that the presence of an imino group at position 2 and a small methyl group at position 6 conferred superior binding characteristics, while bulkier substitutions diminished efficacy due to steric hindrance. Among the pyridine-based analogs, compound 11 showed notable activity, particularly against K. pneumoniae (MIC = 32 µg/mL), with an IC50 of 5.60 ± 0.27 µM and a favorable docking profile. Molecular docking simulations highlighted the critical interactions within the DHFR active site and validated the observed *in-vitro* trends. Overall, compounds 4c and 11 represent promising scaffolds for the development of next-generation DHFR-targeting antimicrobial agents.

INTRODUCTION: Over the past several decades, the excessive use of antibiotics has likely contributed to the development of MDR, thereby significantly compromising their therapeutic efficacy. One of the major public health challenges of the twenty-first century is the emergence and growth of antibiotic-resistant microbial strains, including multidrug-resistant isolates of the ESKAPE pathogens: *Enterococcus faecium*, *Staphylococcus aureus (S. aureus)*, *Klebsiella pneumoniae (K. pneumoniae)*, *Acinetobacter baumannii*, *Pseudomonas aeruginosa*, and *Enterobacter species* [1, 2].

QUICK RESPONSE CODE

DOI: 10.13040/IJPSR.0975-8232.17(1).213-28

This article can be accessed online on www.ijpsr.com

DOI link: https://doi.org/10.13040/IJPSR.0975-8232.17(1).213-28

However, a class of therapeutic compounds have been developed as inhibitors of Dihydrofolate reductase (DHFR) which is an essential enzyme involved in bacterial DNA synthesis [3, 4]. Moreover, heterocyclic compounds featuring pyrimidine and pyridine scaffolds have emerged as one of the most significant classes in medicinal chemistry, garnering substantial attention from researchers in the field. Because they are the fundamental building blocks of many bioactive substances [5], including anti-diabetics [6], anti-histamines [6], anticancers [7], antivirals [7], anticonvulsants [8] and antioxidants [9]. In addition, aminopyrimidine-based compounds have reportedly unveiled antimicrobial activities *via* DHFR inhibition. Trimethoprim (TMP, I) is a well-established antimicrobial agent that exerts its effect by inhibiting dihydrofolate reductase (DHFR). It is a diaminopyrimidine derivative commonly administered in combination with sulfamethoxazole for the treatment of various infections [10]. Numerous studies have reported structural modifications of trimethoprim (TMP) aimed at reducing the emergence of resistance and enhancing its antimicrobial efficacy **Fig. 1.** However, a pyrazole-clubbed aminopyrimidine hybrid (II) has been reported to exhibit greater inhibitory activity against the target enzyme DHFR compared to trimethoprim (TMP), as demonstrated by its lower IC_{50} value relative to that of TMP [11].

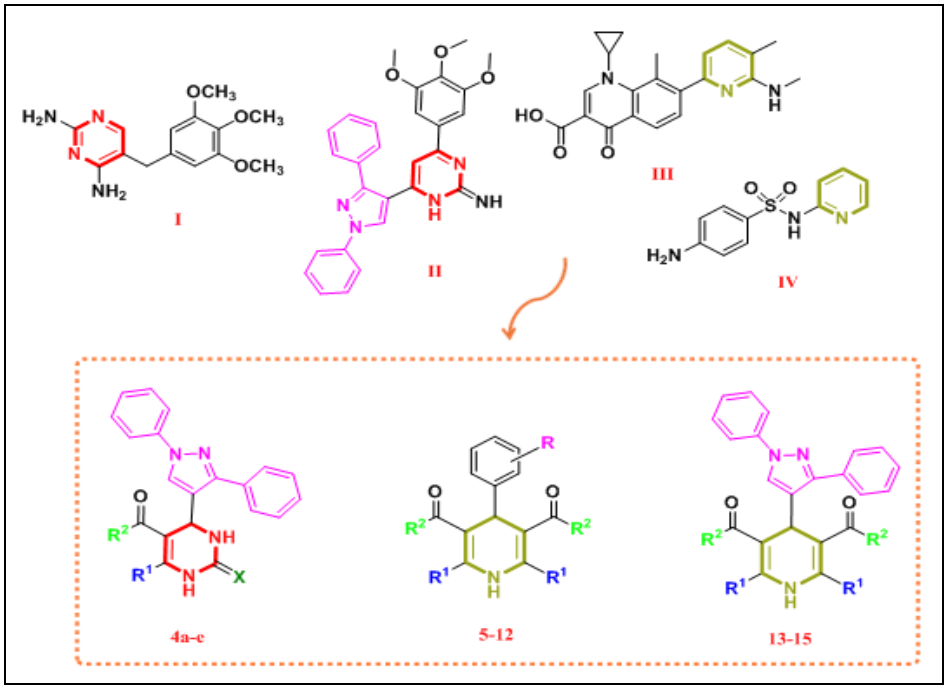

FIG. 1: RATIONALE DESIGN OF THE NEWLY SYNTHESIZED COMPOUNDS (4-15)

However, the rate at which new antibiotics are being developed is far slower than our increasing need for them in the fight against microbial illnesses. Therefore, to treat infections brought on by problematic MDR strains, it is imperative to develop innovative treatment plans and investigate efficient therapeutic alternatives [12]. Therefore, in the last 10 years, the FDA has approved many pyridine-containing antibiotics aiming at inhibition of essential bacterial enzymes, such as Ozenoxacin (III) which has been shown to inhibit DNA gyrase supercoiling activity and bacterial topoisomerase IV in *S. aureus*, [13] and sulfapyridine (IV) which acts as a competitive inhibitor of the bacterial enzyme dihydropteroate synthetase a vital enzyme in bacterial DNA synthesis [14]. Inspired by the previous findings, the goal of the present study was to design new antibacterial and antifungal agents with enhanced inhibitory activity against DHFR and to hamper TMP resistance. To achieve this, tetrahydropyrimidine and pyridine scaffolds were selected for synthesis, each directly linked at the 4-position to either phenyl or diphenylpyrazole moieties, with the objective of generating more structurally rigid analogues compared to TMP. The incorporation of a diphenylpyrazole ring at the 4-position of either a 2-imino or oxo-dihydropyrimidine core, as seen in compounds (4a–e), was undertaken to investigate the influence of ring size and to improve the binding profile.

Alternatively, the tetrahydropyrimidine ring was replaced with a dihydropyridine moiety in compounds (5–15) to generate novel derivatives with potentially enhanced biological activity and reduced toxicity. This modification also aimed to evaluate the structural and functional differences between the two ring systems, as supported by biological assays and computational studies. The *in-vitro* antimicrobial activity of the newly synthesized compounds was investigated against *Escherichia coli (E. coli), K. pneumoniae, S. aureus* and *Candida albicans (C. albicans)*. Additionally, DHFR enzyme inhibitory activity was also determined. Molecular modeling simulations were conducted to identify the possible binding interactions between the target compounds and DHFR enzyme active site.

MATERIALS AND METHODS:

Chemistry: All chemicals, solvents and reagents were purchased from commercial suppliers and used without further purification. Melting points (°C) were recorded using a Stuart melting point apparatus and are uncorrected. IR spectra were recorded on Shimadzu IR-470 spectrometer (υ' in cm^{-1}) using KBr disk at Faculty of Pharmacy and FT-IR using a Bruker FT-IR spectrometer (Invenio S, Germany), Faculty of Science, Mansoura University, Egypt. ^{1}H-NMR and ^{13}C-NMR spectra were recorded on Bruker spectrometer at 400 MHz and 100 MHz, respectively in DMSO-d6 with TMS as internal standard, at Faculty of Pharmacy, Mansoura University, Egypt.The mass spectra were recorded in ESImode (Hewlett Packard 5988 spectrometer)at The Regional Center For Mycology and Biotechnology, Al-Azhar University, Egypt. Elemental analysis was carried out for C, H, and N at the Microanalytical Centre of Cairo University, and they agreed with proposed structures within ± 0.01-0.04% of the calculated values. The Completion of reactions was monitored using thin layer chromatography (TLC) on Silica Gel G60 F-245 (Merck), and the spots were visualized by U.V (366, 245 nm), CH_2Cl_2/MeOH (10:1), and pet. Ether/EtOAc (1:1) or (3:1) were adopted as elution solvents.

General Procedure for Synthesis of diphenyl-pyrazolylpyrimidine (4a-e): Diphenyl pyrazolyl aldehyde [15] (4 mmol) was added to guanidine/urea (1mmol) and mixed with appropriate β-keto ester (1mmol) in ethanol (10ml), with addition of 1-2 drops of concentrated hydrochloric acid. Thereafter, the reaction mixture was let to reflux for 24-48 hrs, and stirred in iced water bath for an additional 6-8 hrs. The formed precipitate was filtered and recrystallized from ethanol.

1-[4-(1, 3-Diphenyl – 1*H* - pyrazol -4-yl)-2-oxo-6-methyl-1, 2, 3,4-tetrahydropyrimidin-5-yl]ethan-1-one (4a): Reddish orange crystals, m.p: 230 ̊C, yield: (67%). IR (cm^{-1}): 1505 (C=N pyrazole), 1602 (C=O), 1664 (C=O), 2971 (aliphatic-CH), 3154 (aromatic-CH), 3357 (NH), 3448 (NH). ^{1}H-NMR (400 MHz, DMSO-d_6), δ: 2.30 (s, 3H, CH_3), 2.43 (s, 3H, CH_3), 5.70 (s, 1H, 4-H), 6.15 (s,1H, pyrazole-H), 7.40-7.51 (m, 5H, phenyl-H), 7.60-7.75 (m, 5H, phenyl-H), 8.35 (s, 1H, NH D_2O-exchangeable), 9.31 (s, 1H, NH D_2O-exchangeable).^{13}C-NMR (100 MHz, DMSO-d_6), δ: 17.7(C-CH_3), 24.4 (C-CH_3), 47.7 (C-4, pyrimidine), 97.9 (C-5, pyrimidine), 104.5 (C-4, pyrazole), 121.1 (C-2, C-6, N-phenyl), 124.9 (C-4, N-phenyl), 126.2 (C-2, C-6, 3-phenyl), 127.1 (C-4, 3-phenyl), 128.8 (C-5, pyrazole), 129.2 (C-3, C-5, 3-phenyl), 130.4 (C-1, N-phenyl), 131.1 (C-1, 3-phenyl), 137.8 (C-3, C-5, N-phenyl), 151.4 (C-6, pyrimidine), 156.4 (C-3, pyrazole), 163.9 (C-2, pyrimidine), 174.3 (C-1, carbonyl). Mass (m/z, %): 207.12 (100), 372.16 (M^+, 23.8). Anal. Calc. For$C_{22}H_{20}N_4O_2$: Calculated %: C, 70.95; H, 5.41; N, 15.04. Found %: C, 70.94; H, 5.40; N, 15.05.

1-[4-(1,3-Diphenyl-1*H*-pyrazol-4-yl)-2-imino-6-methyl-1,2,3,4-tetrahydropyrimidin-5-yl]ethan-1-one (4b): Brown powder, m.p: 205-210 ̊C, yield: (78%). IR (cm^{-1}): 1548 (C=N pyrazole), 1574 (C=N), 1646 (C=O), 2916 (aliphatic-CH), 3147 (aromatic-CH), 3248 (NH), 3332 (NH), 3404 (NH).^{1}H-NMR (400 MHz, DMSO-d_6), δ: 2.22 (s, 3H, CH_3), 3.80 (s, 3H, CH_3), 5.09 (s, 1H, 4-H), 5.92 (s, 1H, pyrazole-H), 7.43-7.45 (m, 5H, phenyl-H), 7.50-7.52 (m,5H, phenyl-H), 7.96 (s, 1H, NH D_2O-exchangeable), 8.02 (s, 1H, NH D_2O-exchangeable), 8.14 (s, 1H, NH D_2O-exchangeable).^{13}C-NMR (100 MHz, DMSO-d_6), **δ:** 19.4 (C-CH_3), 26.8 (C-CH_3), 47.7 (C-4, pyrimidine), 101.2 (C-5, pyrimidine), 110.0 (C-4, pyrazole), 121.1 (C-2, C-6, N-phenyl), 128.8 (C-2, C-6, 3-phenyl), 129.0 (C-4, N-phenyl), 129.6 (C-5, pyrazole), 131.8 (C-4, 3-phenyl), 132.3 (C-3, C-5, 3-phenyl), 134.3 (C-1, N-phenyl), 137.8 (C-1, 3-

phenyl), 138.9 (C-3, C-5, N-phenyl), 143.7 (C-6, pyrimidine), 148.9 (C-3, pyrazole), 152.5 (C-2, pyrimidine). Mass (m/z, %): 71.27 (100), 371.18 (M^+, 63.8). Anal. Calc. For$C_{22}H_{21}N_5O$: Calculated %: C, 71.14; H, 5.70; N, 18.85. Found %: C, 71.16; H, 5.69; N, 18.84.

Ethyl 4-(1,3-diphenyl-1*H*-pyrazol-4-yl)-2-imino-6-methyl-1, 2, 3, 4-tetrahydropyrimidine-5-carboxylate (4c): Dark brown powder, m.p: 210-213 ˚C, yield: (77%). IR (cm^{-1}):1536 (C=N pyrazole), 1597 (C=N), 1706 (ester C=O), 2975 (aliphatic-CH), 3057 (aromatic-CH), 3210 (NH), 3401 (NH), 3571 (NH).^{1}H-NMR (400 MHz, DMSO-d_6), δ:2.38 (t, J = 8.00 Hz, 3H, ester-CH_3), 3.36 (q, J = 8.00 Hz, 2H, ester-CH_2), 3.99 (s, 3H, CH_3), 5.82 (s, 1H, 4-H), 6.25 (s, 1H, pyrazole-H), 7.31-7.49 (m, 5H, phenyl-H), 7.53-7.73 (m, 5H, phenyl-H), 7.99 (s, 1H, NH D_2O-exchangeable), 8.13 (s, 1H, NH D_2O-exchangeable), 8.78 (s, 1H, NH D_2O-exchangeable). ^{13}C-NMR (100 MHz, DMSO-d_6), δ: 19.4 (C-CH_3), 31.2 (C-CH_3), 40.5 (C-CH_2), 87.7 (C-4, pyrimidine), 109.0 (C-4, pyrazole), 118.4 (C-5, pyrimidine), 121.1 (C-2, C-6, N-phenyl), 123.2 (C-5, pyrazole), 123.9 (C-4, N-phenyl), 125.2 (C-4, 3-phenyl), 127.8 (C-2, C-6, 3-phenyl), 130.1 (C-3, C-5, 3-phenyl), 132.3 (C-1, N-phenyl), 136.8 (C-1, 3-phenyl), 139.3 (C-3, C-5, N-phenyl), 141.9 (C-6, pyrimidine), 147.8 (C-3, pyrazole), 161.9 (C-2, pyrimidine), 180.1 (C-ester).Mass (m/z, %): 210.12 (100), 401.19 (M^+, 54.9). Anal. Calc. For $C_{23}H_{23}N_5O_2$: Calculated %: C, 68.81; H, 5.77; N, 17.44. Found %: C, 68.80; H, 5.79; N, 17.43.

Ethyl 4-(1,3-diphenyl-1*H*-pyrazol-4-yl)-2-oxo-6-phenyl - 1, 2, 3, 4 - tetrahydropyrimidine-5-carboxylate (4d): Yellow crystals, m.p : 270 ˚C, yield: (73%). IR (cm^{-1}): 1549 (C=N pyrazole), 1613 (C=O), 1694 (ester C=O), 2958 (aliphatic-CH), 3070 (aromatic-CH), 3220 (NH), 3400 (NH). ^{1}H-NMR (400 MHz, DMSO-d_6), δ: 1.98 (t, J = 8.00 Hz, 3H, ester-CH_3), 2.28 (q, J = 8.00 Hz, 2H, ester-CH_2), 5.45 (s, 1H, 4-H), 6.31 (s, 1H, pyrazole-H), 7.44-7.53 (m, 5H, phenyl-H), 7.77-7.81 (m, 5H, phenyl-H), 7.88-7.90 (m, 5H, phenyl-H), 8.32 (s, 1H, NH D_2O-exchangeable), 9.19 (s, 1H, NH D_2O-exchangeable).^{13}C-NMR (100 MHz, DMSO-d_6), δ: 19.5 (C-CH_3), 46.1 (C-CH_2), 92.9 (C-4, pyrimidine), 107.9 (C-4, pyrazole), 118.4 (C-5, pyrimidine), 120.3 (C-2, C-6, N-phenyl), 122.1 (C-5, pyrazole), 123.2 (C-4, N-phenyl), 124.9 (C-4, 3-phenyl), 125.1 (C-2, C-6, 6-phenyl), 126.8 (C-3, C-5, 6-phenyl), 127.9 (C-1, 6-phenyl), 128.5 (C-4, 6-phenyl), 128.9 (C-2, C-6, 3-phenyl), 129.9 (C-3, C-5, 3-phenyl), 133.4 (C-1, N-phenyl), 139.8 (C-1, 3-phenyl), 142.5 (C-6, pyrimidine), 148.1 (C-3, C-5, N-phenyl), 150.7 (C-3, pyrazole), 152.5 (C-ester), 164.9 (C-2, pyrimidine). Mass (m/z, %): 160.11 (100), 464.19 (M^+, 70.3). Anal. Calc. For $C_{28}H_{24}N_4O_3$: Calculated %: C, 72.40; H, 5.21; N, 12.06. Found %: C, 72.41; H, 5.19; N, 12.05.

Ethyl 4-(1,3-diphenyl-1*H*-pyrazol-4-yl)-2-imino-6-phenyl - 1, 2, 3, 4 – tetrahydropyrimidine – 5 - carboxylate (4e): Pale yellow powder, m.p: 250-255 ˚C, yield: (68%). IR (cm^{-1}): 1534 (C=N pyrazole), 1595 (C=N), 1701 (ester C=O), 2924 (aliphatic-CH), 3054 (aromatic-CH), 3381 (NH), 3571 (NH). ^{1}H-NMR (400 MHz, DMSO-d_6), δ: 1.65 (t, J = 8.00 Hz, 3H, ester-CH_3), 3.00 (q, J = 8.00 Hz, 2H, ester-CH_2), 5.63 (s,1H, 4-H), 5.94 (s, 1H, pyrazole-H), 7.26-7.34 (m, 5H, phenyl-H), 7.46-7.52 (m, 5H, phenyl-H), 7.55-7.70 (m, 5H, phenyl-H), 7.90 (s, 1H, NH D_2O-exchangeable), 8.02 (s, 1H, NH D_2O-exchangeable), 8.30 (s, 1H, NH D_2O-exchangeable). ^{13}C-NMR (100 MHz, DMSO-d_6), δ: 18.5 (C-CH_3), 31.3 (C-CH_2), 103.5 (C-4, pyrazole), 111.1 (C-4, pyrimidine), 114.8 (C-5, pyrimidine), 118.8 (C-2, C-6, N-phenyl),120.1 (C-5, pyrazole), 124.2 (C-4, N-phenyl), 124.9 (C-4, 3-phenyl), 126.4 (C-2, C-6, 6-phenyl), 130.4 (C-3, C-5, 6-phenyl), 132.4 (C-1, 6-phenyl), 134.1 (C-4, 6-phenyl), 135.8 (C-2, C-6, 3-phenyl), 136.9 (C-3, C-5, 3-phenyl), 138.1 (C-1, N-phenyl), 139.9 (C-1, 3-phenyl), 143.7 (C-6, pyrimidine), 147.9 (C-3, C-5, N-phenyl), 159.7 (C-2, pyrimidine), 162.9 (C-3, pyrazole), 180.1 (C-ester).Mass (m/z, %): 63.16 (100), 463.20 (M^+, 70.3). Anal. Calc. For $C_{28}H_{25}N_5O_2$: Calculated %: C, 72.55; H, 5.44; N, 15.1. Found %: C, 72.53; H, 5.46; N, 15.10.

General Procedure for Synthesis of Dihydropyridine Derivatives (5-15): The appropriate aldehyde derivative (5 mmol) was mixed with the β-keto ester derivative (10 mmol) in 100ml rounded bottom flask, and ammonium acetate (7.5 mmol) was added in ethanol (15-20 ml). The reaction mixture was refluxed for 6-12 hrs. The reaction mixture was cooled to room temperature, and 5 ml ethanol was added. Hence,

the resulted precipitate was filtered and recrystallized from ethanol.

1,1'-[4-(2-Hydroxyphenyl)-2, 6-dimethyl-1, 4-dihydropyridine-3, 5-diyl] bis(ethan-1-one) (5): Orange crystals, m.p: 160 ̊C, yield: (88 %). IR (cm^{-1}): 1596 (C=C pyridine), 1641 (C=O), 1672 (C=O), 2974 (aliphatic-CH), 3080 (aromatic-CH), 3188 (NH), 3397 (broad-OH). ^{1}H-NMR (400 MHz, DMSO-d_6), δ: 1.20 (s, 6H, 2,6-CH_3), 2.40 (s, 6H, 3,5-CH_3), 4.08 (s, 1H, 4-H), 7.15 (d, *J* = 8.00 Hz, 1H, 3`-H), 7.36 (d, *J* = 8.00 Hz, 1H, 5`-H), 7.45 (d, *J* = 8.00 Hz, 1H, 6`-H), 7.51 (d, *J* = 8.00 Hz, 1H, 4`-H), 7.98 (s, 1H, NH D_2O-exchangeable), 10.01 (s, 1H, OH D_2O-exchangeable). ^{13}C-NMR (100 MHz, DMSO-d_6), δ: 14.5 (C-CH_3), 27.4 (C-CH_3), 62.8 (C-4, pyridine), 107.3 (C-3, C-5, pyridine), 111.8 (C-3`), 115.1 (C-5`), 120.4 (C-1`), 122.5 (C-6`), 124.3 (C-4`), 128.1 (C-2, C-6, pyridine), 130.5 (C-2`), 145.6 (C-carbonyl). Mass (m/z, %): 80.21 (100), 285.14 (M^+, 88.4). Anal. Calc. For $C_{17}H_{19}NO_3$: Calculated %: C, 71.56; H, 6.71; N, 4.91. Found %: C, 71.54; H, 6.70; N, 4.92.

Diethyl 2, 6-dimethyl-4-(2-nitrophenyl)-1, 4-dihydropyridine-3, 5-dicarboxylate (6): Reddish brownpowder, m.p: 217 ̊C, yield: (66 %). IR (cm^{-1}): 1620 (C=C pyridine), 1690 (ester C=O), 1700 (ester C=O), 2975 (aliphatic-CH), 3050 (aromatic-CH), 3272 (NH). ^{1}H-NMR (400 MHz, DMSO-d_6), δ: 1.75 (s, 6H, 2,6-CH_3), 2.24 (q, *J* = 8.00 Hz, 4H, ester-CH_2), 3.03 (t, *J* = 8.00 Hz, 6H, ester-CH_6), 4.95 (s, 1H, 4-H), 6.57 (d, *J* = 8.00 Hz, 1H, 6`-H), 7.51 (d, *J* = 8.00 Hz, 1H, 3`-H), 7.83 (d, *J* = 8.00 Hz, 2H, 4`-H, 5`-H), 8.54 (s, 1H, NH D_2O-exchangeable).^{13}C-NMR (100 MHz, DMSO-d_6), δ: 14.4 (C-CH_3), 38.5 (C-CH_2), 40.5 (C-CH_3), 61.7 (C-4, pyridine), 123.9 (C-3, C-5, pyridine), 124.8 (C-3`), 126.4 (C-5`), 128.5 (C-1`), 128.9 (C-4`), 129.1 (C-6`), 130.4 (C-2, C-6, pyridine), 139.9 (C-2`), 179.9 (C-ester). Mass (m/z, %): 170.15 (100), 374.15 (M^+, 60.5). Anal. Calc. For $C_{19}H_{22}N_2O_6$: Calculated %: C, 60.95; H, 5.92; N, 7.48. Found %: C, 60.94; H, 5.91; N, 7.49.

Diethyl 4-(4-bromophenyl)-2, 6-diphenyl-1, 4-dihydropyridine-3,5-dicarboxylate (7): Pale yellow crystals, m.p: 212-215 ̊C, yield: (76 %). IR (cm^{-1}): 1596 (C=C pyridine), 1690 (ester C=O), 1722 (ester C=O), 2976 (aliphatic-CH), 3066 (aromatic-CH), 3273 (NH). ^{1}H-NMR (400 MHz, DMSO-d_6), δ: 2.47 (q, *J* = 8.00 Hz, 4H, ester-CH_2), 3.39 (t, *J* = 8.00 Hz, 6H, ester-CH_6), 4.27 (s, 1H, 4-H), 7.14-7.34 (m, 5H, phenyl-H), 7.51-7.62 (m, 5H, phenyl-H), 7.71 (d, *J* = 8.00 Hz, 2H, 2`-H, 6`-H), 7.96 (d, *J* = 8.00 Hz, 2H, 3`-H, 5`-H), 9.82 (s, 1H, NH D_2O-exchangeable). ^{13}C-NMR (100 MHz, DMSO-d_6), δ:14.2 (C-CH_3), 36.3 (C-4, pyridine), 61.7 (C-CH_2), 118.8 (C-3, C-5, pyridine), 120.1 (C-4`), 124.2 (C-2, C-6, 2,6-phenyl), 124.9 (C-4, 2,6-phenyl), 126.6 (C-3, C-5, 2,6-phenyl), 128.9 (C-1, 2,6-phenyl), 130.4 (C-3`, C-5`), 131.5 (C-2`, C-6`), 139.9 (C-2, C-6, pyridine), 162.8 (C-1`), 180.1 (C-ester).Mass (m/z, %): 230.09 (100), 531.11 (M^+, 33.4), 533.10 (M^++2, 37.3). Anal. Calc. For $C_{29}H_{26}BrNO_4$: Calculated %: C, 65.42; H, 4.92; N, 2.63. Found %: C, 65.40; H, 4.91; N, 2.63.

Diethyl 4-(4-chlorophenyl)-2, 6-diphenyl-1, 4-dihydropyridine-3, 5-dicarboxylate (8): Yellow crystals, m.p: 178-181 ̊C, yield: (86 %). IR (cm^{-1}): 1596 (C=C pyridine), 1700 (ester C=O), 1743 (ester C=O), 2927 (aliphatic-CH), 3053 (aromatic-CH), 3399 (NH). ^{1}H-NMR (400 MHz,DMSO-d_6), δ: 2.40 (q, *J* = 8.00 Hz, 4H, ester-CH_2), 3.52 (t, *J* = 8.00 Hz, 6H, ester-CH_6), 4.42 (s, 1H, 4-H), 7.30-7.46 (m, 5H, phenyl-H), 7.53-7.64 (m, 5H, phenyl-H), 7.82 (d, *J* = 8.00 Hz, 2H, 2`-H, 6`-H), 7.99 (d, *J* = 8.00 Hz, 2H, 3`-H, 5`-H), 8.82 (s, 1H, NH D_2O-exchangeable). Mass (m/z, %): 180.16 (100), 487.16 (M^+, 71.4), 489.15 (M^++2, 32). Anal. Calc. For $C_{29}H_{26}ClNO_4$: Calculated %: C, 71.38; H, 5.37; N, 2.87. Found %: C, 71.39; H, 5.38; N, 2.85.

Diethyl 4-(2-nitrophenyl)-2, 6-diphenyl-1, 4-dihydropyridine-3, 5-dicarboxylate (9): Yellow to orange fine powder, m.p: 201-207 ̊C, yield: (80 %). IR (cm^{-1}): 15**97** (C=C pyridine), 1705 (ester C=O), 1744 (ester C=O), 2970 (aliphatic-CH), 3157 (aromatic-CH), 3366 (NH). ^{1}H-NMR (400 MHz, DMSO-d_6), δ: 2.22 (q, *J* = 8.00 Hz, 4H, ester-CH_2), 3.49 (t, *J* = 8.00 Hz, 6H, ester-CH_6), 4.05 (s, 1H, 4-H), 6.44 (d, *J* = 8.00 Hz, 1H, 3`-H), 7.11-7.28 (m, 5H, phenyl-H), 7.40-7.62 (m, 5H, phenyl-H), 7.77 (d, *J* = 8.00 Hz, 1H, 6`-H), 7.92 (d, *J* = 8.00 Hz, 2H, 4`-H, 5`-H), 9.13 (s, 1H, NH D_2O-exchangeable). Mass (m/z, %):92.18 (100), 498.18 (M^+, 61.4). Anal. Calc. For $C_{29}H_{26}N_2O_6$: Calculated %: C, 69.87; H, 5.26; N, 5.62. Found %: C, 69.89; H, 5.28; N, 5.60.

Diethyl 4-(2-hydroxyphenyl)-2, 6-diphenyl-1,4-dihydropyridine-3,5-dicarboxylate (10): Brown powder, m.p : 220 ̊C, yield: (77 %). IR (cm^{-1}): 1613 (C=C pyridine), 1694 (ester C=O), 1755 (ester C=O), 2958 (aliphatic-CH), 3070 (aromatic-CH), 3220 (NH), 3400 (broad OH). ^{1}H-NMR (400 MHz, DMSO-d_6), δ: 2.36 (q, *J* = 8.00 Hz, 4H, ester-CH_2), 3.39 (t, *J* = 8.00 Hz, 6H, ester-CH_6), 4.13 (s, 1H, 4-H), 6.94 (d, *J* = 8.00 Hz, 1H, 3`-H), 7.17 (d, *J* = 8.00 Hz, 1H, 6`-H), 7.66-7.74 (m, 5H, phenyl-H), 7.90-7.93 (m, 5H, phenyl-H), 8.04 (d, *J* = 8.00 Hz, 2H, 4`-H, 5`-H), 8.16 (s, 1H, NH D_2O-exchangeable), 10.31 (s, 1H, OH D_2O-exchangeable). Mass (m/z, %): 110.19 (100), 469.19 (M^+, 71.4). Anal. Calc. For $C_{29}H_{27}NO_5$**:** Calculated %: C, 74.18; H, 5.80; N, 2.98. Found %: C, 74.17; H, 5.81; N, 2.97.

Diethyl 4-(4-hydroxyphenyl)-2, 6-diphenyl-1,4-dihydropyridine-3,5-dicarboxylate (11): Yellow crystals, m.p: 220 ̊C, yield:(82 %). IR (cm^{-1}): 1605 (C=C pyridine), 1694 (ester C=O), 1723 (ester C=O), 2931 (aliphatic-CH), 3050 (aromatic-CH), 3200 (NH), 3327 (broad-OH). ^{1}H-NMR (400 MHz, DMSO-d_6), δ: 2.32 (q, *J* = 8.00 Hz, 4H, ester-CH_2), 3.32 (t, *J* = 8.00 Hz, 6H, ester-CH_6), 4.14 (s, 1H, 4-H), 7.17 (d, *J* = 8.00 Hz, 2H, 2`-H, 6`-H), 7.31 (d, *J* = 8.00 Hz, 2H, 3`-H, 5`-H), 7.45-7.67 (m, 5H, phenyl-H), 7.83-7.89 (m, 5H, phenyl-H), 8.46 (s, 1H, NH D_2O-exchangeable), 10.22 (s, 1H, OH D_2O-exchangeable). ^{13}C-NMR (100 MHz, DMSO-d_6), δ: 11.3 (C-CH_3), 32.2 (C-4, pyridine), 56.5 (C-CH_2), 118.9 (C-3, C-5, pyridine), 119.9 (C-4`), 124.8 (C-2, C-6, 2,6-phenyl), 126.2 (C-4, 2,6-phenyl), 127.3 (C-3, C-5, 2,6-phenyl), 128.5 (C-1, 2,6-phenyl), 129.2 (C-3`, C-5`), 130.4 (C-2`, C-6`), 139.4 (C-2, C-6, pyridine), 154.6 (C-1`), 179.6 (C-ester). Mass (m/z, %): 90.14 (100), 469.19 (M^+, 81.4). Anal. Calc. For $C_{29}H_{27}NO_5$: Calculated %: C, 74.18; H, 5.80; N, 2.98.Found %: C, 74.17; H, 5.81; N, 2.97.

Diethyl 4-(2-methoxyphenyl)-2, 6-diphenyl-1,4-dihydropyridine-3, 5-dicarboxylate (12): Dark yellow crystals, m.p: 220-224 ̊C, yield: (83%). IR (cm^{-1}): 1597 (C=C pyridine), 1719 (ester C=O), 1740 (ester C=O), 2926 (aliphatic-CH), 3070 (aromatic-CH), 3316 (NH). ^{1}H-NMR (400 MHz, DMSO-d_6), δ: 2.48 (q, *J* = 8.00 Hz, 4H, ester-CH_2), 2.81 (s, 3H, methoxy-CH_3), 3.31 (t, *J* = 8.00 Hz, 6H, ester-CH_6), 3.98 (s, 1H, 4-H), 7.14 (d, *J* = 8.00 Hz, 1H, 3`-H), 7.18 (d, *J* = 8.00 Hz, 1H, 6`-H), 7.36-7.43 (m, 5H, phenyl-H), 7.57-7.63 (m, 5H, phenyl-H), 7.79 (d, *J* = 8.00 Hz, 2H, 4`-H, 5`-H), 8.17 (s, 1H, NH D_2O-exchangeable). ^{13}C-NMR (100 MHz, DMSO-d_6), δ: 16.3 (C-CH_3), 26.9 (C-4, pyridine), 41.4 (C-CH_2), 118.6 (C-3, C-5, pyridine), 119.6 (C-4`), 122.1 (C-2, C-6, 2,6-phenyl), 124.1 (C-4, 2,6-phenyl), 125.3 (C-3`), 126.2 (C-3, C-5, 2,6-phenyl), 128.4 (C-1, 2,6-phenyl), 129.0 (C-2`), 129.9 (C-6`), 130.3 (C-5`), 139.9 (C-2, C-6, pyridine), 151.6 (C-1`), 179.9 (O-CH_3), 181.6 (C-ester). Mass (m/z, %): 180.11 (100), 483.21 (M^+, 72.4). Anal. Calc. For $C_{30}H_{29}NO_5$: Calculated %: C, 74.52; H, 6.05; N, 2.90. Found %: C, 74.51; H, 6.06; N, 2.91.

1,1'-[4-(1, 3-Diphenyl-1*H*-pyrazol-4-yl)-2, 6-dimethyl-1, 4-dihydropyridine-3, 5-diyl] bis (ethan-1-one) (13): Dark red to black crystals, m.p: 205 ̊C, yield: (91%).**IR (cm^{-1}):** 1573 (C=N pyrazole), 1610 (C=C pyridine), 1653 (C=O), 1685 (C=O), 2928 (aliphatic-CH), 3060 (aromatic-CH), 3388 (NH). ^{1}H-NMR (400 MHz, DMSO-d_6), δ: 1.90 (s, 6H, 2,6-CH_3), 2.40 (s, 6H, 3,5-CH_3), 4.17 (s, 1H, 4-H), 6.59 (s, 1H, pyrazole-H), 7.20-7.37 (m, 5H, phenyl-H), 7.43-7.62 (m, 5H, phenyl-H), 9.36 (s, 1H, NH D_2O-exchangeable). ^{13}C-NMR (100 MHz, DMSO-d_6), δ: 20.4 (C-CH_3), 21.5 (C-CH_3), 68.8 (C-4, pyridine), 117.2 (C-4, pyrazole), 118.9 (C-3, C-5, pyridine), 119.4 (C-2, C-6, N-phenyl), 121.8 (C-5, pyrazole), 123.4 (C-4, N-phenyl), 124.0 (C-4, 3-phenyl), 124.8 (C-2, C-6, 3-phenyl), 125.5 (C-3, C-5, 3-phenyl), 126.5 (C-1, 3-phenyl), 128.9 (C-2, C-6, pyridine), 130.4 (C-1, N-phenyl), 139.9 (C-3, C-5, N-phenyl), 154.6 (C-3, pyrazole), 181.5 (C-carbonyl). Mass (m/z, %): 102.12 (100), 411.20 (M^+, 88.1). Anal. Calc. For $C_{26}H_{25}N_3O_2$: Calculated %: C, 75.89; H, 6.12; N, 10.21.Found %: C, 75.88; H, 6.10; N, 10.23.

Diethyl 4-(1, 3-diphenyl-1*H*-pyrazol-4-yl)-2,6-dimethyl-1,4-dihydropyridine-3, 5-dicarboxylate (14): Off-white powder, m.p: 201-207 ̊C, yield: (84%). IR (cm^{-1}): 1563 (C=C pyrazole), 1607 (C=C pyridine), 1711 (ester C=O), 1739 (ester C=O), 2978 (aliphatic-CH), 3021 (aromatic-CH), 3218 (NH).^{1}H-NMR (400 MHz, DMSO-d_6), δ: 1.51 (s, 6H, 2,6-CH_3), 2.25 (q, *J* = 8.00 Hz, 4H, ester-CH_2), 3.36 (t, *J* = 8.00 Hz, 6H, ester-CH_6), 5.78 (s, 1H, 4-H), 6.19 (s, 1H, pyrazole-H), 7.06-7.18 (m, 5H, phenyl-H), 7.30-7.55 (m, 5H, phenyl-H), 8.61 (s,

1H, NH D_2O-exchangeable). Mass (m/z, %): 90.26 (100), 471.22 (M^+, 83.3). Anal. Calc. For $C_{28}H_{29}N_3O_4$: Calculated %: C, 71.32; H, 6.20; N, 8.91. Found %: C, 71.33; H, 6.19; N, 8.90.

Diethyl 4-(1, 3-diphenyl-1*H*-pyrazol-4-yl)-2, 6-diphenyl-1,4-dihydropyridine-3,5-dicarboxylate (15): Dark brown powder, m.p: 260-265 ̊C, yield: (76%). IR (cm^{-1}): 1575 (C=N pyrazole), 1620 (C=C pyridine), 1702 (ester C=O), 1739 (C=O), 2932 (aliphatic-CH), 3057 (aromatic-CH), 3269 (NH). ^{1}H-NMR (400 MHz, DMSO-d_6), δ: 2.48 (q, *J* = 8.00 Hz, 4H, ester-CH_2), 3.39 (t, *J* = 8.00 Hz, 6H, ester-CH_6), 3.99 (s, 1H, 4-H), 5.34 (s, 1H, pyrazole-H), 7.18-7.26 (m, 5H, phenyl-H), 7.46-7.54 (m, 5H, Ar-CH), 7.68-7.76 (m, 5H, Ar-CH)7.97-8.01 (m, 5H, phenyl-H), 9.02 (s, 1H, NH D_2O-exchangeable). ^{13}C-NMR (100 MHz, DMSO-d_6), δ: 13.1 (C-CH_3), 31.2 (C-4, pyridine), 48.8 (C-CH_2), 104.8 (C-4, pyrazole), 113.7 (C-3, C-5, pyridine), 118.8 (C-2, C-6, N-phenyl), 119.4 (C-5, pyrazole),121.9 (C-4, N-phenyl), 122.3 (C-4, 3-phenyl), 124.9 (C-2, C-6, 3-phenyl), 125.8 (C-3, C-5, 3-phenyl), 126.5 (C-1, 3-phenyl), 127.5 (C-3, C-5, 2,6-phenyl), 128.9 (C-1, 2,6-phenyl), 131.5 (C-2, C-6, pyridine), 130.4 (C-1, N-phenyl), 139.6 (C-2, C-6, 2,6-phenyl),142.7 (C-3, C-5, N-phenyl), 144.8 (C-4, 2,6-phenyl), 154.8 (C-3, pyrazole), 180.6 (C-carbonyl).Mass (m/z, %): 291.21 (100), 595.18 (M^+, 71.1).Anal. Calc. for $C_{38}H_{33}N_3O_4$: Calculated %: C, 76.62; H, 5.58; N, 7.05. Found %: C, 76.64; H, 5.59; N, 7.04.

Biological Screening:

***In vitro* Antimicrobial Activity:**

Bacterial Inoculum Preparation and Determination of Inhibition Zone (IZ) by Disc Diffusion Technique: The antimicrobial activity of the synthesized compounds was estimated using the disc diffusion technique described by Clinical and Laboratory Standards Institute guidelines (CLSI) [16]. All solvents and chemicals were purchased from Sigma Aldrich company-UK. *E. coli*, *K. pneumoniae*, *S. aureus*, and *C. albicans* were obtained from the culture collection of the Department of Microbiology and Immunology, Delta University for Science and Technology, Egypt. Nutrient broth, Muller-Hinton sabouraud dextrose agar, and resazurine were obtained from Oxoid, Hampshire, UK. Separate colonies of each isolatefrom the overnight culture were suspended in nutrient broth for bacteria or Sabouraud dextrose agar for fungi. After overnight incubation at 37ºC, turbidity was adjusted to 0.5 MacFarland standard (1.5×10^8 CFU/mL), and five wells were made onto the surface of the dried Mueller Hinton agar (MHA). Plates were inoculated using cotton swabs in three different directions then the wells were filled with the solution of the tested compounds prepared in a concentration equal to 10 µg/ µL. Finally, the inoculated agar plates were incubated at 37ºC for 16-18 hrs and diameters of the produced inhibition zones were measured to the closest full millimeter using calipers placed on the back of the upright petri dish and interpreted according to **CLSI** in comparison to trimethoprim [16].

Determination of the Minimal Inhibitory Concentration (MIC): MICs for the most promising compounds were determined according to the broth microdilution method described CLSI [16]. Using a 96-well microtiter plate, each well contained 100 µL of double-strength Mueller-Hinton broth for supporting the bacterial growth or Sabouraud dextrose broth for the fungi, including a growth control well and a sterility control (uninoculated) well. The tested compounds were added twice the desired final concentration, and a two-fold serial dilution was performed. Bacterial and fungal strains were initially grown on nutrient agar and sabouraud agar for 24 h at 37°C, and isolated colonies were used to prepare a saline suspension with turbidity equivalent to a 0.5 McFarland standard (1.5×10^8 CFU/mL).

Then, 100 µL of bacterial saline suspension was added to each well except for sterility control wells. MIC was defined as the lowest concentration at which there is no visual bacterial growth. It was detected by using resazurin dye that undergoes colorimetric change in response to cellular metabolic reduction producing a pink, fluorescent resofurin product [16, 17].

Dihydrofolate Reductase (DHFR) Inhibition Assay: The inhibitory effect assay of the newly synthesized compounds against DHFR enzyme was described in our previous reports [11, 18] and conducted as detailed in the BioVision manufacturer's protocol, taking TMP as a standard drug instead of Methotrexate [19, 20].

Molecular Modeling Simulation:

Retrieval and Preparation of Macromolecules: The crystal structure of *S. aureus* F98Y DHFR complexed with TMP(PDB:3FRB) [21] at a resolution of 2.00 Å was retrieved from the Protein Data Bank (https://www.rcsb.org/). All water molecules were removed, and all hydrogenatoms were added to the crystal 3D structure of each protein with their standard geometry followed by their energy minimization.

Preparation of the Ligands: All the newly synthesized were drawn into Marvin Sketch of Marvin suite (http://www.chemaxon.com) followed by the generation of the lowest energy conformer for each. The dock module of MOE (Molecular Operating Environment) version MOE 2024.06 was adopted in running molecular modeling simulation studies. The prepared thymol and thymoquinone ligands in MDL Molfile (*.mol) format, were docked onto the rigid binding pocket in the active site of the aforementioned protein using flexible ligand mode. Poses from ligand conformation were generated from the placement phase. The force field-based scoring function GBVI/WSA ΔG.[22], was employed to calculate the free binding energy of the ligand from a certain pose.

RESULTS AND DISCUSSION:

Chemistry: Synthesis of diphenyl-pyrazolyl-dihydropyrimidin-2(1*H*)-one derivatives (4a-e) are shown in **Fig. 2**.

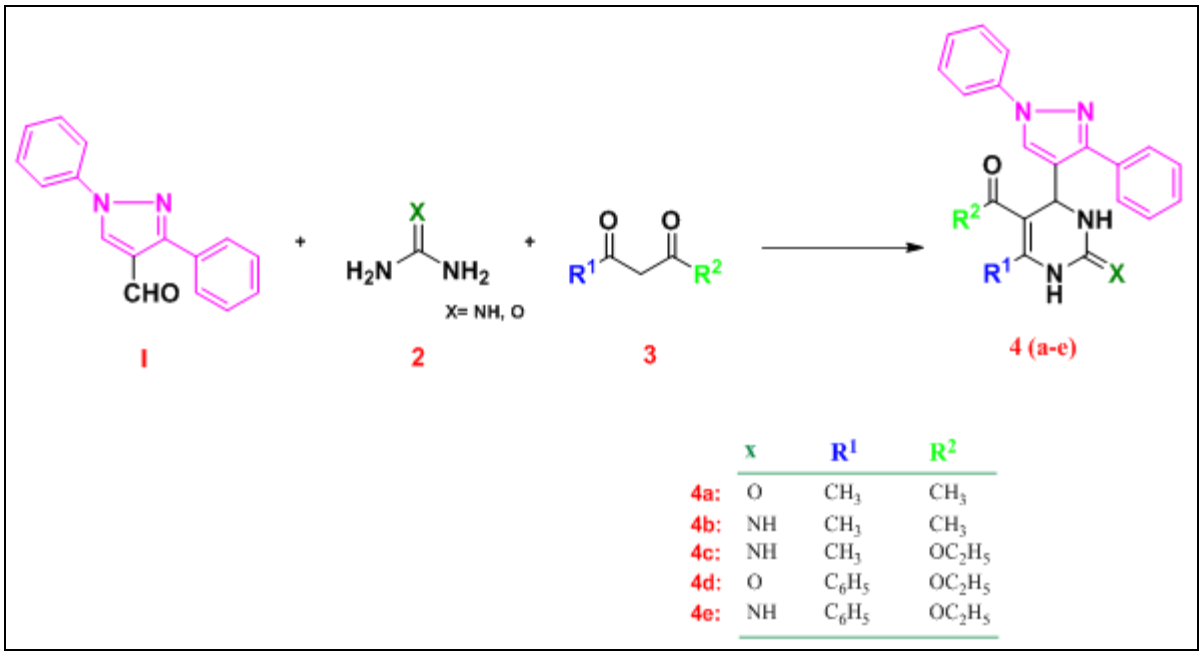

	x	R^1	R^2
4a:	O	CH_3	CH_3
4b:	NH	CH_3	CH_3
4c:	NH	CH_3	OC_2H_5
4d:	O	C_6H_5	OC_2H_5
4e:	NH	C_6H_5	OC_2H_5

FIG. 2: SYNTHESIS OF DIPHENYL-PYRAZOLYLDIHYDROPYRIMIDIN-2(1*H*)-ONE (4A-E)

In the present study, the traditional Biginelli synthetic method was employed to obtain the target hybrids (4a-e) with satisfactory yield and purity. Moreover, diphenyl-pyrazolyldihydropyrimidin-2(1*H*)-one series were synthesized using 3-(aryl)-1-phenyl - 1*H* – pyrazole – 4 - carbaldehydes [15], ethylacetoacetate and guanidinium chloride or guanidine was reported by Shah *et a.l* [23] and diphenylpyrazole carbaldehyde derivative was synthesized ae reported using Vilsmeier-haack reaction [24-26]. The presence of a characteristic singlet signal corresponding to the pyrazole proton, observed at approximately δ = 6.92–7.31 ppm, represents a key spectral feature of the target analogues.

Besides, characteristic peaks corresponding to classical aromatic protons were observed in the ^{1}H-NMR spectra. Furthermore, a singlet peak corresponding to the three protons of the 6-CH_3 group in compounds 4a–c was observed at approximately δ = 3.0–4.0 ppm. In addition, the infrared spectra exhibited characteristic absorption bands for the ester carbonyl group in the range of 1694–1706 cm^{-1}, as observed in compounds 4c–e. A distinct stretching band corresponding to the C=N bond of the pyrazole ring was detected at 1584 cm^{-1}, while an additional amide carbonyl absorption band appeared at 1602 cm^{-1} in compound 4a. Still, distinctive absorption bands attributed to the ketone functional group were

observed at 1664 cm^{-1} and 1646 cm^{-1} in compounds 4a and 4b, respectively. NH stretching vibrations were also detected in the range of 3248–3404 cm^{-1}. Also, the ^{13}C-NMR spectra revealed the characteristic signals for the C-2 carbon of the pyrimidine ring in compounds 4a–e, observed in the range of δ = 152.5–163.9 ppm. However, the carbonyl group of the ester moiety in compounds 4c–e was detected at δ = 180.1 ppm. Still, another distinctive signal corresponding to the C-3 carbon of the pyrazole ring was observed in the range of δ = 148.9–150.1 ppm.

Whereas **Fig. 3:** represents the synthesis of dihydropyridine derivatives (5-15).

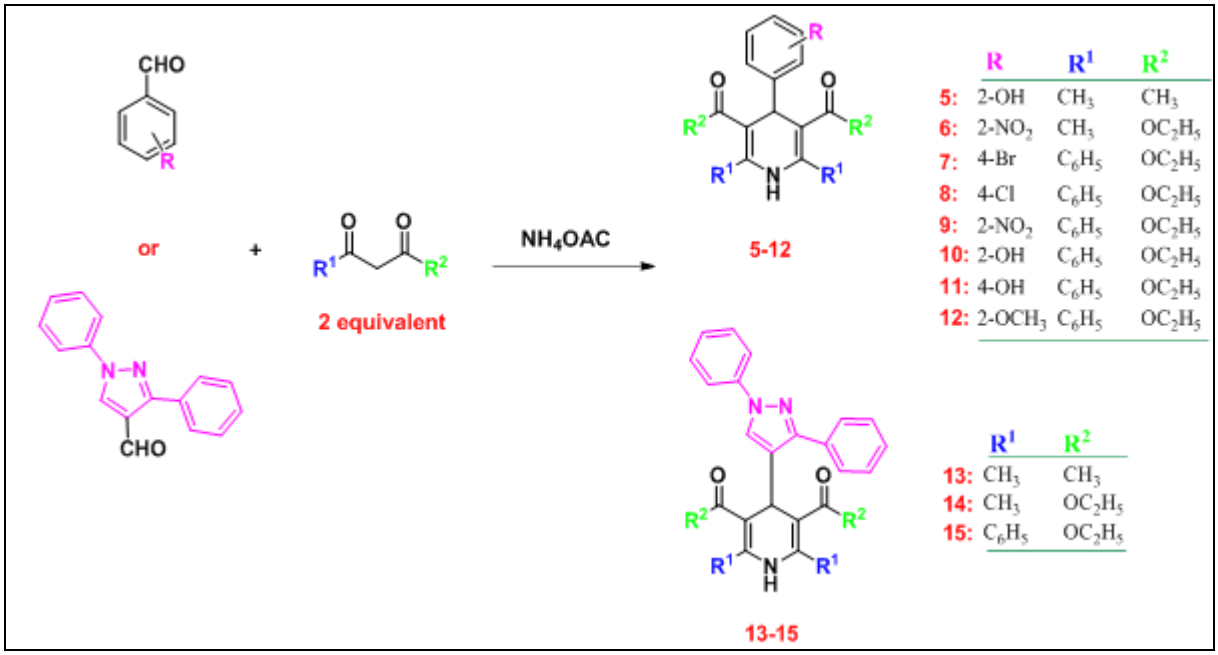

FIG. 3: SYNTHESIS OF DIHYDROPYRIDINE COMPOUNDS (5-15)

The Hantzsch reaction, is a well-established method for the synthesis of dihydropyridines (DHPs) [27] . The reaction is proposed to proceed *via* a Knoevenagel condensation product, which serves as a key intermediate. Another crucial intermediate is an ester enamine, formed through the condensation of a second equivalent of the β-ketoester with ammonia. Subsequent condensation between these two intermediates leads to the formation of the 1,4-dihydropyridine derivative. Overall, the reaction involves four components: one molecule of ammonia, one aldehyde, and two β-ketoesters, culminating in the synthesis of 1,4-dihydropyridines. Aldehydes, both aliphatic and aromatic, make good Hantzsch reaction substrates. Ammonium hydroxide, ammonium bicarbonate, and ammonium acetate are the three possible sources of ammonia compounds in the Hantzsch process [28]. The Hantzsch reaction can use β-ketoester and its derivatives or variations, such as diacetone, ethyl acetoacetate, dimedone, and so on; the two β-ketoesters can be the same or different, depending on whether the reaction is symmetric or asymmetric. Different conditions were tried to optimize the products yield, such as adding ammonium acetate and acetyl acetone [29].

Upon comparing the pyrimidine rings in the previously discussed compounds with the pyridine rings in the series 5–15, a distinct NH stretching band of the pyridine moiety was observed in the range of 3200–3300 cm^{-1}. Additionally, the C=C stretching vibrations characteristic of the pyridine ring appeared at approximately 1596–1620 cm^{-1}. A broad OH stretching band was also detected at 3397 cm^{-1} in compound 5. However, the C=O stretching bands appeared within the expected range of 1700–1755 cm^{-1} for ester functionalities, while ketone groups, as observed in compounds 5 and 13, exhibited stretching bands in the range of 1641–1685 cm^{-1}.Additionally, characteristic band for NH proton of pyridine ring in the ^{1}H-NMR charts in the range of δ=8-9 ppm, with the characteristic peaks of symmetrical ester protons.

Biological Screening:

***In-vitro* Antimicrobial Activity:**

Determination of the Inhibition Zones (IZ): The results presented in **Table1**indicated that compound 4b exhibited moderate activity exclusively against *K. pneumoniae*, while compounds 4d and 4e demonstrated intermediate activity against both *K. pneumoniae* and *S. aureus.* Additionally, compound 4e exhibited strong antifungal activity. In contrast, compound 4a demonstrated moderate inhibitory effects against both *K. pneumoniae* and *C. albicans*. Notably, compound 4c was effective against *S. aureus* and *C. albicans*, showing a remarkable inhibitory activity.

TABLE 1: ANTIMICROBIAL ACTIVITY OF THE TARGET COMPOUNDS 4A-E USING AGAR DIFFUSION METHOD

Compound no.	Diameter of Inhibition Zone (I.Z) (mm)			
	E. coli	*K. pneumoniae*	*S. aureus*	*C. albicans*
4a	– (R)	13 (I)	– (R)	13 (I)
4b	– (R)	11(I)	– (R)	– (R)
4c	– (R)	– (R)	22 (S)	25 (S)
4d	– (R)	11(I)	12 (I)	– (R)
4e	– (R)	13 (I)	12 (I)	17 (S)
Levofloxacin	32	25	– (R)	30

*Results are interpreted as resistant (R) if I.Z ≤ 10 mm, intermediate (I) if I.Z (11-16) mm, and sensitive (S) if I.Z ≥ 16 mm.

Among the newly synthesized dihydropyridine series, as presented in **Table 2**, compound 6 demonstrated the highest efficacy against *K. pneumoniae*, *S. aureus,* and *C. albicans.* Moreover, compound 13 exhibited moderate activity against *K. pneumoniae*, *S. aureus*, and *C. albicans*. In contrast, compound 10 demonstrated good activity against *C. albicans* and moderate activity against *K. pneumoniae*. Conspicuously, *E. coli* exhibited resistance to all synthesized derivatives except compound 11, which showed moderate activity against *E. coli* and strong activity against *K. pneumoniae*. Compounds 7, 8, 9, and 14 were selectively active against *K. pneumoniae*, while compounds 12 and 15 showed no detectable activity against any of the tested microorganisms.

TABLE 2: ANTIMICROBIAL ACTIVITY OF THE TARGET COMPOUNDS 5-15 USING AGAR DIFFUSION METHOD

Compound no.	Diameter of Inhibition Zone (I.Z) (mm)			
	E. coli	*K. pneumoniae*	*S. aureus*	*C. albicans*
5	– (R)	– (R)	– (R)	– (R)
6	– (R)	12 (I)	13 (I)	19 (S)
7	– (R)	11 (I)	–(R)	– (R)
8	– (R)	11 (I)	– (R)	– (R)
9	– (R)	11 (I)	–(R)	– (R)
10	– (R)	13 (I)	– (R)	16 (S)
11	13 (I)	16 (S)	– (R)	– (R)
12	– (R)	– (R)	– (R)	– (R)
13	– (R)	14 (I)	13 (I)	13 (I)
14	– (R)	11 (I)	–(R)	– (R)
15	– (R)	– (R)	– (R)	– (R)
Levofloxacin	32	25	– (R)	30

*Results are interpreted as resistant (R) if I.Z ≤ 10 mm, intermediate (I) if I.Z (11-16) mm, and sensitive (S) if I.Z ≥ 16 mm.

Quantitative Assay for Determination of the Minimal Inhibitory Concentration (MIC): The most active compounds were further evaluated to determine their minimum inhibitory concentrations (MICs) using the broth microdilution method, to confirm and quantify their antimicrobial efficacy. The data presented in **Table 3** demonstrated that compound 4c exhibited broad-spectrum activity against all tested microorganisms, recording the lowest MIC values against *S. aureus* and *C. albicans*. Likewise, Compound 6 exhibited selective activity, with MIC values of 16 µg/mL against *S. aureus* and 32 µg/mL against *C. albicans*, while demonstrating limited activity

against *E. coli* and *K. pneumoniae.*Moreover, compound 11 demonstrated strong antimicrobial activity against both Gram-positive and Gram-negative bacteria, including *K. pneumoniae* and *S. aureus* (MIC = 16 µg/mL), as well as notable antifungal activity against *C. albicans* (MIC = 64 µg/mL). Moreover, compound 4e demonstrated notable antibacterial activity against *S. aureus* (MIC = 32 µg/mL) and exhibited moderate antifungal activity against *C. albicans* (MIC = 64 µg/mL). Alternatively, Compounds 7 and 9 exhibited significant antifungal activity against *C. albicans*, while demonstrating only weak antibacterial activity against both Gram-positive and Gram-negative strains compared to reference drug Levofloxacin.

TABLE 3: MICS OF THE MOST PROMISING COMPOUNDS AGAINST *E. COLI, K. PNEUMONIAE, S. AUREUS* AND *C. ALBICANS*

Compound no.	MIC (µg/ mL)			
	E. coli	***K. pneumoniae***	***S. aureus***	***C. albicans***
4c	128	128	16	16
4e	> 1,024	> 1,024	32	64
5	> 1,024	> 1,024	> 1,024	32
6	512	1,024	16	32
7	> 1,024	> 1,024	> 1,024	64
9	> 1,024	128	> 1,024	64
10	> 1,024	64	> 1,024	32
11	128	32	32	64
13	> 1,024	> 1,024	> 1,024	128
14	> 1,024	> 1,024	> 1,024	128
Levofloxacin	128	128	1,024	16

Dihydrofolate Reductase (DHFR) Inhibition Assay: The *in-vitro* DHFR inhibition assay was conducted to evaluate the potential of the newly synthesized compounds as DHFR inhibitors, using trimethoprim (TMP) as the reference standard (IC_{50} = 5.33 ± 0.26 µM). The calculated IC_{50} values expressed in micromolar concentrations were listed in **Table 4** and graphically illustrated in **Fig. 4**. The IC_{50} values of the tested compounds ranged from 5.53 ± 0.26 µM to 7.06 ± 0.33 µM, indicating varying degrees of inhibitory activity.

Among the diphenylpyrazolyl derivatives, compound 4c demonstrated the most promising DHFR inhibitory effect (IC_{50} = 5.53 ± 0.26 µM), approaching that of TMP, followed closely by compounds 4a, 4b, and 4e with IC_{50} values of 5.56 ± 0.23 µM, 5.62 ± 0.27 µM, and 5.60 ± 0.28 µM, respectively.

These findings suggested that substitution patterns on the pyrazole-linked tetrahydropyrimidine core contribute positively to DHFR inhibition. Compound 4d, however, showed slightly reduced activity (IC_{50} = 6.00 ± 0.28 µM), possibly due to steric or electronic effects associated with its specific substituents. The pyridine-based derivatives (5–15) displayed a broader range of inhibitory activity. Notably, compounds 10, 8, and 11 exhibited strong inhibition with IC_{50} values of 5.53 ± 0.27 µM, 5.62 ± 0.27 µM, and 5.60 ± 0.27 µM, respectively, indicating that these analogues are among the most effective in this series.

Compounds 5, 7, and 9 showed moderate inhibition (IC_{50} = 5.77 ± 0.28 µM, 5.95 ± 0.28 µM, and 5.87 ± 0.27 µM, respectively), suggesting that minor structural variations within the pyridine scaffold can influence binding affinity.

Conversely, compounds 6, 13, 14, and 15 exhibited weaker inhibitory effects with IC_{50} values ranging from 6.65 ± 0.32 µM to 7.06 ± 0.33 µM, highlighting that certain substitutions may reduce interaction with the DHFR active site or adversely affect conformational stability.

Overall, several compounds, particularly 4c, 10, and 11, displayed IC_{50} values comparable to or only slightly higher than TMP, indicating their potential as promising DHFR inhibitors. The observed variations across the series underscore the importance of scaffold selection and functional group positioning in optimizing DHFR inhibitory activity.

TABLE 4: RESULTS OF THE *IN-VITRO* DHFR INHIBITION ASSAY OF ALL NEWLY SYNTHESIZED COMPOUNDS

Ligand	DHFR inhibition IC_{50} (µM)[a]	Docking score (Kcal/mol)
4a	5.56±0.23	-11.0830041
4b	5.62±0.27	-11.3363848
4c	5.53±0.26	-12.1143856
4d	6.00±0.28	-10.5044861
4e	5.60±0.28	-11.2797203
5	5.77±0.28	-10.5665207
6	6.93±0.34	-10.0303125
7	5.95±0.28	-10.9119101
8	5.62±0.27	-10.4413643
9	5.87±0.27	-9.38088894
10	5.53±0.27	-10.5951414
11	5.60±0.27	-11.6284666
12	5.68±0.25	-9.85770702
13	6.65±0.32	-11.0176182
14	6.89±0.33	-9.1018343
15	7.06±0.33	-8.84663486
TMP	5.33±0.26	-11.6648388

[a]IC_{50} (µM): Expressed as mean± S.D

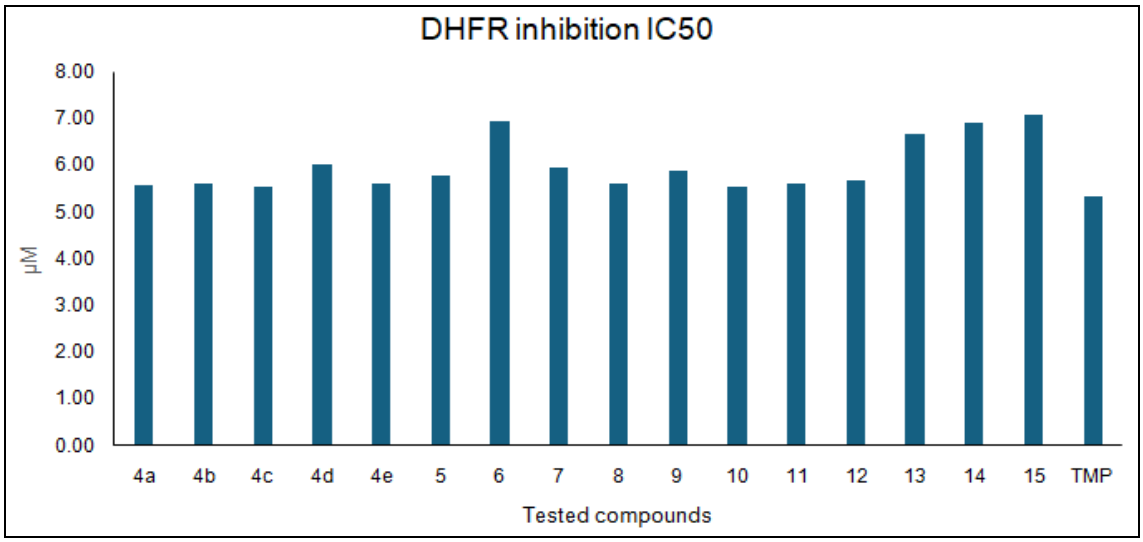

FIG. 4: DHFR INHIBITION CHART OF THE TESTED COMPOUNDS VERSUS TMP (REFERENCE DRUG) EXPRESSED AS IC_{50} (µM)

Molecular Modeling Simulation: Molecular modeling involves the application of theoretical and computational methods to simulate the interaction of a molecule within a receptor's binding site, with the objective of elucidating its binding characteristics and assessing the ligand's affinity for its target receptor protein [30]. A series of ligands (compounds 4a–15) were docked into the TMP binding site within the crystal structure of the *S. aureus* F98Y DHFR mutant, using the crystal structure complexed with TMP as the reference ligand (PDB ID: 3FRB), as depicted in Supp. **Fig. 1.** The docking scores of all compounds are listed in Supp. **Table 1** and are expressed in kcal/mol, reflect the predicted binding free energy and thus provide an indication of the relative binding strengths of the ligands to the target protein. Among the tested compounds, compound 4c exhibited the most favorable docking score (-12.114 kcal/mol), surpassing even that of the reference inhibitor TMP (-11.665 kcal/mol). As shown in **Fig. 5**, in compound 4c, two H-bonds were established between sp^3-hybridized nitrogen atom and the hydrogen atom attached to sp^2-hybridized nitrogen within the pyrimidine ring on the ligand side, and the conserved amino acid residues Tyr98 and Gly94 on the receptor side, respectively.

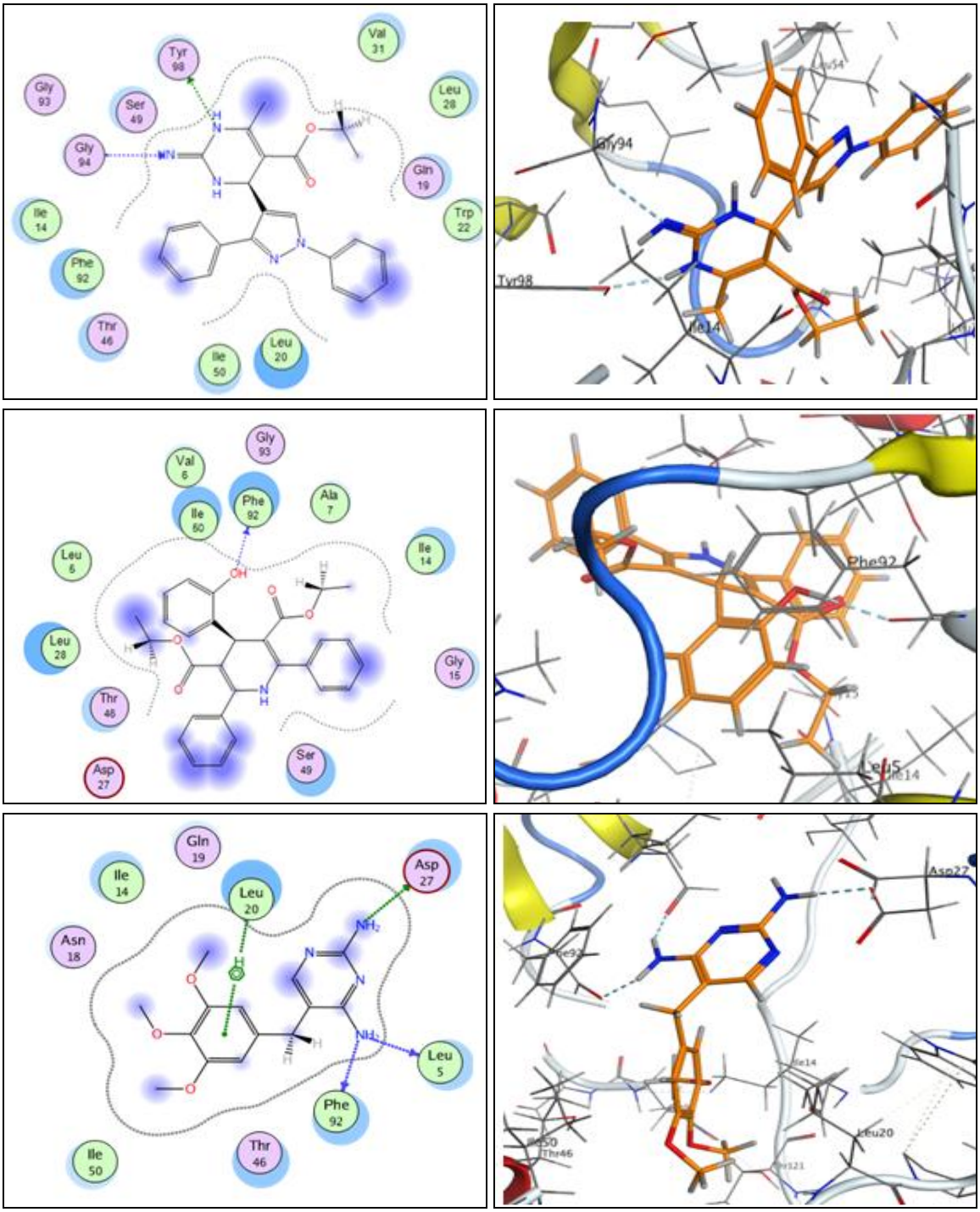

FIG. 5: PUTATIVE BINDING MODES OF COMPOUND 4C (UPPER PANEL), COMPOUND 10 (MIDDLE PANEL) AND TMP (LOWER PANEL) WITH TMP BINDING SITE IN *S. AUREUS* F98Y DHFR (PDB: 3FRB) RECEPTOR

This suggests that 4c may have a higher binding affinity to the F98Y DHFR mutant than TMP, potentially translating into enhanced inhibitory activity. Moreover, the hydrophobic/ hydrophilic interactions indicated by the cyan-shaded amino acid residues from active site side, and blue shaded regions of the ligand, enhanced molecular recognition and the overall stability of receptor/and complex. Compounds 11 (-11.628 kcal/mol), 4b (-11.336 kcal/mol), and 4e (-11.280 kcal/mol) also showed comparable or slightly improved binding affinities relative to TMP, indicating their potential as strong DHFR inhibitors. The majority of the ligands displayed docking scores within the range of -10 to -11 kcal/mol, indicating generally good binding potential. Compounds such as 4a, 7, 10, and 13 all fall within this range, with scores between -10.6 and -11.1 kcal/mol.

These values suggest that structural modifications within this subset could further optimize binding interactions. For instance, the enhanced binding affinity of compound 4b compared to compound 4 acould be attributed to the substitution of an oxygen atom with a nitrogen atom at position 2. In contrast, modifications at position 2 of the phenyl ring attached to position 4 of the pyridine core, such as hydroxyl groups in compounds 5 and 10, or NO_2 and methoxy groups in compounds 6 and 12 respectively, negatively affected the ligand's fit within the active site, thereby reducing binding efficiency. Conversely, compounds 14 and 15 exhibited the weakest binding affinities within the series, with docking scores of -9.102 kcal/mol and -8.847 kcal/mol, respectively. These lower binding energies are likely due to suboptimal interactions within the enzyme's active site and unfavorable conformational constraints. The increased ring size, resulting from substitution of the phenyl group at position 4 with a diphenylpyrazole moiety, likely caused fluctuations in the ligand's orientation within the binding pocket, leading to diminished binding energies despite the presence of hydrogen and arene–H bonding interactions **Fig. 1.**

Interestingly, compound 7, the *para*-brominated analogue, exhibited notable hydrophobic and hydrophilic interactions within the active site and uniquely formed a characteristic halogen bond [31, 32] between the bromine atom and the conserved amino acid residue Asp27. Noteworthy, the inclusion of the F98Y mutation in the DHFR enzyme is particularly relevant, as this point mutation is known to confer resistance to TMP. Therefore, ligands that exhibit equal or superior binding affinities compared to TMP may overcome this resistance mechanism. The promising performance of compound 4c and others highlights their potential as leads for the development of next-generation DHFR inhibitors active against resistant *S. aureus* strains. Principally, after the validation of these compounds through *in-vitro* assays that confirmed the binding stability and biological activity of these compounds, the docking results provided a strong foundation for prioritizing compounds 4c, 11, 4b, and 4e for further investigations.

CONCLUSION: The integrated biological assessment of the synthesized compounds, including antimicrobial MIC assays, DHFR enzyme inhibition studies, and molecular docking simulations, facilitated a comprehensive structure–activity relationship (SAR) analysis across two distinct series: the pyrazolyl-pyrimidines (4a–4e) and the pyridine-based derivatives (5–15). This evaluation provided insight into how subtle structural modifications influence antimicrobial potency and DHFR binding efficiency. In the pyrazolyl-pyrimidine series, compound 4c demonstrated the most potent antimicrobial activity, exhibiting low MIC values against *S. aureus* and *C. albicans* (16 µg/mL), alongside moderate efficacy against Gram-negative strains (128 µg/mL). This notable activity is attributed to specific structural features, including a methyl group at position 6, an imino group at position 2, and an *N*-substituted diphenylpyrazole at position 4 of the pyrimidine ring. These features collectively promote favorable hydrogen bonding and hydrophobic interactions within the DHFR active site, while maintaining overall molecular planarity and compactness conducive to cellular uptake. In contrast, compound 4e, although structurally related to 4c, showed substantially reduced activity, particularly against Gram-negative bacteria (MIC >1,024 µg/mL), and only modest effects against *S. aureus* and *C. albicans* (MIC = 32 and 64 µg/mL, respectively). The reduced efficacy of 4e is likely a consequence of its bulkier phenyl substituent at position 6 and the presence of a carbonyl (oxo) group at position 2, both of which may introduce steric hindrance, reduce hydrogen-bonding capacity, and impair membrane permeability. A similar trend was observed in the pyridine-based series. Compound 11 emerged as the most active, with MIC values of 32 µg/mL against *K. pneumoniae* and 128 µg/mL against *E. coli*. Its relatively compact and balanced structure appears to support favorable positioning within the DHFR binding pocket and sufficient cell penetration. In contrast, compound 15, characterized by a large diphenylpyrazole substituent, was the least active of the entire study, with MIC values exceeding 1,024 µg/mL against all tested organisms. The poor activity of 15 is attributed to excessive steric bulk and molecular rigidity, which likely disrupt optimal binding and hinder cellular entry. Biochemical and computational analyses further supported the antimicrobial findings. Compound 4c again led the

pyrazolyl-pyrimidine series, showing the lowest IC_{50} (5.53 μM) for DHFR inhibition and the most favorable docking score (–12.114 kcal/mol), even surpassing that of the reference drug trimethoprim. Docking studies confirmed that 4c establishes two key hydrogen bonds with Gly94 and Tyr98, with its ethyl ester and diphenylpyrazole moieties contributing to optimal fit and stable interactions. Conversely, compound 4d was the least potent in enzymatic terms, with an IC_{50} of 6.00 μM and a relatively weak docking score (–10.504 kcal/mol), likely due to the presence of a phenyl group at position 6 that compromises binding orientation and reduces electronic complementarity.

In the pyridine series, compound 11 exhibited both potent DHFR inhibition (IC_{50} = 5.60 μM) and a strong docking score (–11.628 kcal/mol), suggesting that its molecular architecture effectively balances binding site compatibility and physicochemical properties. By contrast, compound **15** showed the weakest enzymatic inhibition (IC_{50} = 7.06 μM) and the lowest docking score (–8.847 kcal/mol), consistent with its bulky structure and poor antimicrobial activity. Across both scaffold classes, consistent SAR trends could be delineated. Compounds bearing planar, compact, and moderately polarizable substituents capable of engaging in hydrogen bonding and π–stacking interactions demonstrated enhanced DHFR binding and antimicrobial efficacy. In contrast, the presence of bulky, sterically hindering groups, particularly at critical positions such as the 6-position of the pyrimidine ring or the 4-position of the pyridine core, was associated with reduced biological activity, likely due to unfavorable binding geometries and impaired cell penetration. Furthermore, electronic effects from substituents at various positions modulated ligand affinity by influencing the compatibility of the molecule's electron distribution with that of the DHFR active site.

In brief, the pyrazolyl-pyrimidine scaffold, as exemplified by compound 4c, emerged as the most promising chemotype due to its superior performance across antimicrobial, enzymatic, and docking evaluations. While compound 11 from the pyridine series also demonstrated favorable properties, its activity was generally lower than that of 4c. These findings affirm DHFR as a validated target for antimicrobial intervention and highlight compounds 4c and 11 as strong leads for further optimization.

ACKNOWLEDGMENT: We are so grateful to all members of the "Drug Discovery and Development unit", faculty of pharmacy, Delta University for Science and Technology, for providing us with some chemicals and helping us in conducting *in-vitro* and *in-vivo* assays. Additionally, we hereby acknowledge Department of Pharmaceutical Organic Chemistry, Faculty of pharmacy, Mansoura University, for conducting molecular modelling simulation studies.

Supplementary Information: The Supporting Information is associated with this article and includes ^{1}H-NMR, ^{13}C-NMR and IR spectral images of all final compounds in addition to the supplementary tables and figures of molecular docking scores and docking poses.

CONFLICT OF INTEREST: The authors declare no conflict of interest.

REFERENCES:

1. Mancuso G, Midiri A, Gerace E and Biondo C: Bacterial antibiotic resistance: the most critical pathogens. Pathogens 2021; 10(10): 1310.
2. Rani A, Saini KC, Bast F, Varjani S, Mehariya S, Bhatia SK, Sharma N and Funk C: A review on microbial products and their perspective application as antimicrobial agents. Biomolecules 2021; 11: 1860.
3. Azzam R, Essam R and Elgemeie G: Design, Synthesis, and Antimicrobial Evaluation of a New Series of N - Sulfonamide 2-Pyridones as Dual Inhibitors of DHPS and DHFR Enzymes. ACS Omega 2020; 5(18): 10401.
4. Sehrawat R, Rathee P, Khatkar S, Akkol E, Khayatkashani M, Nabavi SM and Khatkar A: Dihydrofolate Reductase (DHFR) Inhibitors: A Comprehensive Review. Current Medicinal Chemistry 2024; 31(7): 799.
5. Marinescu M: Biginelli reaction mediated synthesis of antimicrobial pyrimidine derivatives and their therapeutic properties. Molecules. 2021; 26(19): 6022.
6. Qadir T, Amin A, Sharma PK, Jeelani I and Abe H: A review on medicinally important heterocyclic compounds. The Open Medicinal Chemistry Journal 2022; 16(1).
7. Kumar S, Deep A and Narasimhan B: A review on synthesis, anticancer and antiviral potentials of pyrimidine derivatives. Current Bioactive Compounds 2019; 15: 289-303.
8. Shu VA, Eni DB and Ntie-Kang F: A survey of isatin hybrids and their biological properties. Molecular Diversity 2025; 29(2): 1737-60.
9. Nair N, Majeed J, Pandey P, Sweety R and Thakur R: Antioxidant potential of pyrimidine derivatives against oxidative stress. Indian Journal of Pharmaceutical Sciences 2022; 84.

10. Mubeen B, Ansar AN, Rasool R, Ullah I, Imam SS, Alshehri S, Ghoneim MM, Alzarea SI, Nadeem MS and Kazmi I: Nanotechnology as a novel approach in combating microbes providing an alternative to antibiotics. Antibiotics 2021; 10(12): 1473.
11. Mansour B, El-Sherbeny MA, Al-Omary FA, Saber S, Ramadan HA, El-Baz AM, Mourad AA and Abdel-Aziz NI: New Pyrazole-clubbed pyrimidine or pyrazoline hybrids as Anti-methicillin-resistant Staphylococcus aureus agents: design, synthesis, *in-vitro* and *in-vivo* evaluation, and Molecular modeling Simulation. ACS Omega 2023; 8(46): 44250.
12. Hiremath SM, Suvitha A, Patil NR, Hiremath CS, Khemalapure SS, Pattanayak SK, Negalurmath VS, Obelannavar K, Armaković SJ and Armaković S: Synthesis of 5-(5-methyl-benzofuran-3-ylmethyl)-3H-[1, 3, 4] oxadiazole-2-thione and investigation of its spectroscopic, reactivity, optoelectronic and drug likeness properties by combined computational and experimental approach. Spectrochimica Acta Part A: Molecular and Biomolecular Spectroscopy 2018; 205: 95-110.
13. Vila J, Hebert AA, Torrelo A, López Y, Tato M, García-Castillo M and Cantón R: Ozenoxacin: a review of preclinical and clinical efficacy. Expert Review of Anti-infective Therapy 2019; 17: 159-168.
14. Theobald RJ: Sulfapyridine☆. In Reference Module in Biomedical Sciences; Elsevier 2016.
15. Mansour B, El-Sherbeny MA, Al-Omary FAM, Saber S, Ramadan HA, El-Baz AM, Mourad AAE and Abdel-Aziz NI: New pyrazole-clubbed pyrimidine or pyrazoline hybrids as anti-methicillin-resistant *Staphylococcus aureus* agents: design, synthesis, *in-vitro* and *in-vivo* evaluation, and molecular modeling simulation. ACS Omega 2023; 8: 44250-44264.
16. Kadry AA, El-Antrawy MA and El-Ganiny AM: Management of clinical infections of Escherichia coli by new β-lactam/β-lactamase inhibitor combinations. Iranian Journal of Microbiology 2022; 14(4): 466.
17. Kamiloglu S, Sari G, Ozdal T and Capanoglu E: Guidelines for cell viability assays. Food Frontiers 2020; 1(3): 332-49.
18. Omar AM, Alswah M, Ahmed HEA, Bayoumi AH, El-Gamal KM, El-Morsy A, Ghiaty A, Afifi TH, Sherbiny FF, Mohammed AS and Mansour BA: Antimicrobial screening and pharmacokinetic profiling of novel phenyl-[1,2,4]triazolo[4,3-a]quinoxaline analogues targeting DHFR and E. coli DNA gyrase B. Bioorg Chem 2020; 96: 10.
19. Riyadh SM, El-Motairi SA, Ahmed HE, Khalil KD and Habib ESE: Synthesis, biological evaluation, and molecular docking of novel thiazoles and [1, 3, 4] thiadiazoles incorporating sulfonamide group as DHFR Inhibitors. Chemistry & Biodiversity 2018; 15: 1800231.
20. Zhao Y, Zou S, Huo D, Hou C, Yang M, Li J and Bian M: Simple and sensitive fluorescence sensor for methotrexate detection based on the inner filter effect of N, S co-doped carbon quantum dots. Analytica Chimica Acta 2019; 1047: 179-87.
21. Muñoz KA, Ulrich RJ, Vasan AK, Sinclair M, Wen PC, Holmes JR, Lee HY, Hung CC, Fields CJ, Tajkhorshid E and Lau GW: A Gram-negative-selective antibiotic that spares the gut microbiome. Nature 2024; 630(8016): 429-36.
22. Onufriev AV and Case DA: Generalized born implicit solvent models for biomolecules. Annual Review of Biophysics 2019; 48(1): 275-96.
23. Ragab A, Fouad SA, Ali OA, Ahmed EM, Ali AM, Askar AA and Ammar YA: Sulfaguanidine hybrid with some new pyridine-2-one derivatives: Design, synthesis, and antimicrobial activity against multidrug-resistant bacteria as dual DNA gyrase and DHFR inhibitors. Antibiotics 2021; 10(2): 162.
24. Shamsi F, Hasan P, Queen A, Hussain A, Khan P, Zeya B, King HM, Rana S, Garrison J, Alajmi MF and Rizvi MM: Synthesis and SAR studies of novel 1, 2, 4-oxadiazole-sulfonamide based compounds as potential anticancer agents for colorectal cancer therapy. Bioorganic Chemistry 2020; 98: 103754.
25. Nandurkar Y, Bhoye MR, Maliwal D, Pissurlenkar RR, Chavan A, Katade S and Mhaske PC: Synthesis, biological screening and *in-silico* studies of new N-phenyl-4-(1, 3-diaryl-1H-pyrazol-4-yl) thiazol-2-amine derivatives as potential antifungal and antitubercular agents. European Journal of Medicinal Chemistry 2023; 258: 115548.
26. Yoshimura A, Saito A, Yusubov MS and Zhdankin VV: Synthesis of oxazoline and oxazole derivatives by hypervalent-iodine-mediated oxidative cycloaddition reactions. Synthesis 2020; 52(16): 2299-310.
27. Faisca Phillips AM and Pombeiro AJ: Applications of hantzsch esters in organocatalytic enantioselective synthesis. Catalysts 2023; 13(2): 419.
28. Somprasong S , Castiñeira Reis M and Harutyunyan SR: Grignard Reagent Addition to Pyridinium Salts: A Catalytic Approach to Chiral 1, 4-Dihydropyridines. ACS Catalysis 2024; 14(17): 13030-9.
29. Parthiban A and Makam P: 1, 4-Dihydropyridine: Synthetic advances, medicinal and insecticidal properties. RSC Advances 2022; 12(45): 29253-90.
30. Gomaa SE, Abbas HA, Mohamed FA, Ali MA, Ibrahim TM, Abdel Halim AS, Alghamdi MA, Mansour B, Chaudhary AA and Elkelish A. Boufahja F: The anti-staphylococcal fusidic acid as an efflux pump inhibitor combined with fluconazole against vaginal candidiasis in mouse model. BMC microbiology 2024; 24(1): 54.
31. Mansour B, Bayoumi WA, El-Sayed MA, Abouzeid LA and Massoud MA: *In-vitro* cytotoxicity and docking study of novel symmetric and asymmetric dihydropyridines and pyridines as EGFR tyrosine kinase inhibitors. Chemical Biology & Drug Design 2022; 100(1): 121.
32. El-Abd AO, Bayomi SM, El-Damasy AK, Mansour B, Abdel-Aziz NI and El-Sherbeny MA: Synthesis and molecular docking study of new thiazole derivatives as potential tubulin polymerization inhibitors. ACS Omega 2022; 7(37): 33599.

How to cite this article:
Sherif MM, Mansour B, El-Antrawy MA, Badr SMI and Nasr MNA: Targeting dihydrofolate reductase (DHFR) enzyme: synthesis, *in-vitro* biological evaluation, and molecular modelling of novel tetrahydropyrimidine and dihydropyridine derivatives. Int J Pharm Sci & Res 2026; 17(1): 213-28. doi: 10.13040/IJPSR.0975-8232.17(1).213-28.